Proceedings of the ASME 2014 Pressure Vessels & Piping Conference
PVP2014
July 20-24, 2014, Anaheim, California, USA

PVP2014-28340

Palladium Hydride Atomic Potentials for Hydrogen Storage/Separation

Y.H. Park
MECHANICAL & AEROSPACE ENGINEERING DEPT.
New Mexico State University
LAS CRUCES, NM 88003, U.S.A.

I. Hijazi
DEPARTMENT OF MECHANICAL ENGINEERING
Marshall University
HUNTINGTON, WV 25755, U.S.A.

ABSTRACT

Palladium is capable of storing a large atomic percent of hydrogen at room temperature and allows for hydrogen to diffuse with a high mobility. These unique properties make it an efficient storage medium for hydrogen and hydrogen isotopes, such as tritium, a byproduct of nuclear reaction. Palladium thus can be used for applications where fast diffusion and large storage density are important. Better understanding of molecular level phenomena such as hydride phase transformation in the metal and the effect of defects in the materials provides clues to designing metal hydrides that perform better. Atomic simulations are useful in the evaluation of palladium-hydrogen systems as changes in composition can be more easily explored than with experiments. In this paper, we present the palladium hydride potentials to investigate and identify the relevant physical mechanisms necessary to describe the absorption of hydrogen within a metal lattice.

1. INTRODUCTION

Considerable effort has been devoted to palladium as to its unique hydrogen storage behavior. Palladium is capable of storing a large atomic percent of hydrogen at room temperature [1]. This property enables many applications including hydrogen storage for clean portable energy, new refrigerator designs, catalytic converters, and nuclear radiation adsorption [2-5]. One problem with using palladium is that addition of hydrogen to palladium, as it is for many metals, significantly degrades their properties by reducing ductility and increasing susceptibility to fatigue and corrosion [6]. This is further complicated by the presence of a miscibility gap in the palladium-hydrogen system at room temperature, which results in the separation of the material into a low hydrogen (α) phase, and a high hydrogen (β) phase [7]. For some metals there is a structural phase transformation of the metal lattice in passing from the α to the β phase, but in palladium there is only a change in the lattice constant of the fcc lattice [8]. Palladium hydride may be considered an interstitial alloy, PdH_x, $0 \le x \le 1$, where octahedral sites of the fcc metal lattice are occupied by hydrogen.

Understanding physical phenomena is critical to predict the time evolution (aging behavior) of palladium hydride material properties. Atomistic simulations are useful in the evaluation of palladium hydride systems. In this paper, molecular dynamics (MD) simulations are used to evaluate palladium hydride systems as changes in composition can be more easily explored than with experiments. The EAM potential has been used to successfully study the effects of helium bubbles in palladium matrix [9, 10]. In this paper, the properties of palladium hydrides are predicted by Embedded Atom Method (EAM) interatomic potential for a large range of compositions. The simulated hydrides give a qualitative representation of material behaviors for PdH systems.

2. COMPUTATIONAL METHODS

2.1 Embedded Atom Method

To describe a model of palladium hydride from a microscopic description of the system, we use embedded-atom-method (EAM) potentials to represent the interactions. In the EAM the potential energy E_{pot} of the system can be written as [11]:

$$E_{\text{pot}} = \sum_{i=1}^{N} F_i(\rho_i) + \frac{1}{2}\sum_{i=1}^{N}\sum_{\substack{j=1 \\ j\neq 1}}^{N} \phi_{ij}(r_{ij}) \tag{1}$$

$$\rho_i = \sum_{j\neq i}^{N} f_j(r_{ij}) \tag{2}$$

where ϕ_{ij} is a two-body central potential between atoms i and j, $F_i(\rho_i)$ is an embedding energy at site of atom i in an electron density ρ_i, f_j is the electron density of atom j as a function of distance from its center, and , r_{ij} is the separation distance between atoms i and j. The complete potential is defined by an embedding function for each species F_{Pd}, F_{H} and three pair potentials $\phi_{\text{Pd-Pd}}$, $\phi_{\text{Pd-H}}$, and $\phi_{\text{H-H}}$ as follows:

$$\begin{aligned} E_{\text{pot}} &= E_{pot,Pd} + E_{pot,H} \\ &= \sum_{i=1}^{N} F_{Pd,i}(\rho_{Pd,i}) + \frac{1}{2}\sum_{i=1}^{N}\sum_{\substack{j=1 \\ j\neq i}}^{N} \phi_{Pd-Pd,ij}(r_{ij}) + \frac{1}{2}\sum_{i=1}^{N}\sum_{\substack{j=1 \\ j\neq i}}^{N} \phi_{Pd-H,ij}(r_{ij}) \\ &+ \sum_{i=1}^{N} F_{H,i}(\rho_{H,i}) + \frac{1}{2}\sum_{i=1}^{N}\sum_{\substack{j=1 \\ j\neq i}}^{N} \phi_{H-Pd,ij}(r_{ij}) + \frac{1}{2}\sum_{i=1}^{N}\sum_{\substack{j=1 \\ j\neq i}}^{N} \phi_{H-H,ij}(r_{ij}) \end{aligned} \tag{3}$$

where ϕ_{Pd-H} and ϕ_{H-Pd} take the same form. ϕ_{Pd-H} In Eq. (3), atomic electron densities are defined by

$$\begin{aligned} \rho_{Pd,i} &= \rho_{Pd-Pd,i} + \rho_{Pd-H,i} \\ &= \sum_{j(\neq i)}^{N_{Pd-Pd}} f_e e^{-\chi(r_{ij}-r_e)} + \sum_{j(\neq i)}^{N_{Pd-H}} f_H e^{-\delta_H r_{ij}} \end{aligned} \tag{4}$$

$$\rho_{H,i} = \rho_{H-Pd,i} + \rho_{H-H,i} = \sum_{j(\neq i)}^{N_{H-Pd}} f_e e^{-\chi(r_{ij}-r_e)} + \sum_{j(\neq i)}^{N_{H-H}} f_H e^{-\delta_H r_{ij}} \quad (5)$$

For pure palladium, the embedded-atom-method (EAM) potential developed by the authors [12] is used:

$$F(\rho) = -F_0\left[1-\eta\ln\left(\frac{\rho}{\rho_e}\right)\right]\left(\frac{\rho}{\rho_e}\right)^{\eta} \quad (6)$$

$$f = f_e e^{-\chi(r-r_e)} \quad (7)$$

$$\phi = -\phi_e\left[1+\delta(r/r_e-1)\right]e^{-\beta(r/r_e-1)} \quad (8)$$

where F_0 is constant and f_e is a scaling factor. Six adjustable parameters χ, ϕ_e, δ, β, η, ρ_e are given in Table 1.

Table 1. Fitting parameters for pure Pd

χ	ϕ_e	δ	β	η	ρ_e
3.7960	0.2119	8.7056	7.1238	0.5678	11.5774

With the palladium potential known, a hydrogen potential and a cross-pair potential between palladium and hydrogen need to be developed. In this paper, the same general form of embedded atom potential developed by the authors is proposed for hydrogen and the cross-pair potential in order to obtain consistent results. Hydrogen potential is then approximated by

$$\phi = -\phi_{HH}\left[1+\delta_{HH}(r/r_{HH}-1)\right]e^{-\beta_{HH}(r/r_{HH}-1)} \quad (9)$$

$$f = f_H e^{-\chi_{HH}(r-r_{HH})} \quad (10)$$

$$F(\rho) = -F_{HH}\left[1-\eta_{HH}\ln\left(\frac{\rho}{\rho_{HH}}\right)\right]\left(\frac{\rho}{\rho_{HH}}\right)^{\eta_{HH}} \quad (11)$$

The cross-pair potential between palladium and hydrogen is approximated by

$$\phi = -\phi_{PdH}\left[1+\delta_{PdH}(r/r_{PdH}-1)\right]e^{-\beta_{PdH}(r/r_{PdH}-1)} \quad (12)$$

2.2 Elastic constants

The equations relating the equilibrium properties such as cohesive energy and the linear elastic constants can be obtained by applying an infinitesimal homogeneous strain to a perfect crystal at equilibrium [13]:

$$E = E\big|_0 + \left.\frac{\partial E}{\partial a_i}\right|_0 u_i + \frac{1}{2}\left.\frac{\partial E}{\partial a_i a_k}\right|_0 u_i u_k + \ldots \quad (13)$$

where u_i is a Cartesian component of the displacement vector, a_1, a_2, a_3 are the lengths of the edges of the computational cell. The elastic constant C_{ij} is defined as

$$C_{ij} = \frac{1}{V}\frac{\partial^2 E_{pot}}{\partial\varepsilon_i\partial\varepsilon_j} \quad (14)$$

where ε_i and ε_j (i,j=1,2,…,6) are strains represented by the contracted notation. Cubic crystals have three independent constants C_{11}, C_{12}, and C_{44} and they can be derived as follows:

$$C_{11} = \frac{1}{\Omega_e}\left\{F''(\rho^e)\left[\sum_i \frac{(r_{i1}^e)^2}{r_i^e}f'(r_i^e)\right]^2 + F'(\rho^e)\sum_i \frac{(r_{i1}^e)^4}{(r_i^e)^2}\left(f''(r_i^e)-\frac{f'(r_i^e)}{r_i^e}\right) + F'(\rho^e)\sum_i \frac{(r_{i1}^e)^2}{r_i^e}f'(r_i^e)\right\} + \frac{1}{2\Omega_e}\left\{\sum_i \frac{(r_{i1}^e)^4}{(r_i^e)^2}\left(\phi''(r_i^e)-\frac{\phi'(r_i^e)}{r_i^e}\right)+\sum_i \frac{(r_{i1}^e)^2}{r_i^e}\phi'(r_i^e)\right\} \quad (15)$$

$$C_{12} = \frac{1}{\Omega_e}\left\{F''(\rho^e)\left[\sum_i \frac{(r_{i1}^e)^2}{r_i^e}f'(r_i^e)\right]\left[\sum_i \frac{(r_{i2}^e)^2}{r_i^e}f'(r_i^e)\right] + F'(\rho^e)\sum_i \frac{(r_{i1}^e)^2(r_{i2}^e)^2}{(r_i^e)^2}\left(f''(r_i^e)-\frac{f'(r_i^e)}{r_i^e}\right) + \frac{1}{2\Omega_e}\left\{\sum_i \frac{(r_{i1}^e)^4}{(r_i^e)^2}\left(\phi''(r_i^e)-\frac{\phi'(r_i^e)}{r_i^e}\right)\right\} \quad (16)$$

$$C_{44} = \frac{1}{\Omega_e}\left\{F'(\rho^e)\sum_i \frac{(r_{i2}^e)^2(r_{i3}^e)^2}{(r_i^e)^2}\left(f''(r_i^e)-\frac{f'(r_i^e)}{r_i^e}\right) + \frac{1}{2}\sum_i \frac{(r_{i2}^e)^2(r_{i3}^e)^2}{(r_i^e)^2}\left(\phi''(r_i^e)-\frac{\phi'(r_i^e)}{r_i^e}\right)\right\} \quad (17)$$

2.3 Gibbs free energy mixing

In order for a Pd-H interatomic potential to be applicable to the entire hydrogen composition range $0 \le x \le 1$, it must be capable of predicting the miscibility gap. The phase miscibility is determined by the Gibbs free energy of mixing per atom as a function of composition in units of mole fraction. The Gibbs free energy of mixing is expressed as

$$\Delta G^{mix} = \Delta H^{mix} - \Delta S^{mix}\cdot T \quad (18)$$

where ΔH^{mix} and ΔS^{mix} are enthalpy and entropy of mixing per atom respectively. For the process of forming PdH_x from two reference materials Pd and PdH, the heat of mixing can be defined by [14, 15]

$$\Delta H^{mix} = E_{PdHx} - 2X\cdot E_{PdH} - (1-2X)\cdot E_{Pd} \quad (19)$$

where $X=x/(1+x)$ is mole fraction, E_{PdH}, E_{Pd}, and E_{PdHx} are cohesive energies for PdH, Pd, and PdH_x. The entropy of mixing can be approximated by the change of the configurational entropy. The PdH_x lattice is composed of two sublattices occupied by palladium and hydrogen atoms respectively. The hydrogen sublattices can be viewed as forming a substituional H-vacancy alloy. The total configurational entropy per atom is then

$$\Delta S = -\frac{k[x\cdot\ln(x)+(1-x)\ln(1-x)]}{1+x} \quad (20)$$

where k is Boltzman constant. An entropy of mixing can be expressed using mole fraction as

$$\Delta S^{mix} = -k\left[X \cdot \ln\frac{X}{1-X} + (1-2X)\ln\frac{1-2X}{1-X} \right] \qquad (21)$$

Equations (18), (19), and (22) define a Gibbs free energy of mixing.

2.4 Fitting Procedure

Parameters for EAM potential functions are determined using a constrained nonlinear optimization procedure to minimize the root-square deviation between the calculated and experimental data. Parameters for a pure Pd system, can be found in [12]. Experimental data used for fitting consist of the equilibrium lattice constant, the cohesive energy, heat of mixing, $B=(C_{11}+2C_{12})/3$ and shear modulus $C'=(C_{11}-C_{12})/2$ and C_{44}. Four octahedral (OC) crystals $PdH_{0.25}$, $PdH_{0.5}$, $PdH_{0.75}$, and $PdH_{1.0}$, two tetrahedral (TE) crystals $PdH_{0.25}H_{0.25}$ and $PdH_{0.375}H_{0.375}$, and one fcc hydrogen crystal Pd_0H were considered. The desired properties of the TE structures were simply chosen to ensure that they are less stable than the corresponding (i.e., the same composition) OC structures.

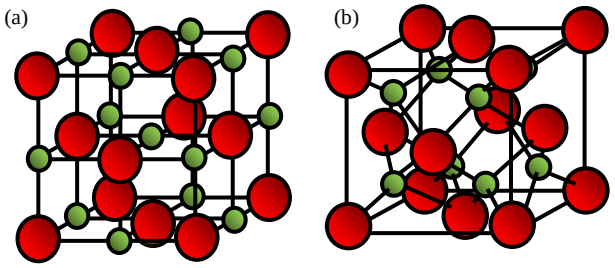

Figure 1. PdH_x structure with hydrogen at (a) octahedral sites and (b) tetrahedral sites

Parameters χ_{HH}, ϕ_{HH}, δ_{HH}, β_{HH}, η_{HH}, ρ_{HH}, r_{HH}, f_H, and F_{HH} appear in the hydrogen potential. The cross-pair potential between palladium and hydrogen has four parameters ϕ_{PdH}, δ_{PdH}, β_{PdH}, and r_{PdH}. The fitted parameters obtained are listed in Tables 2 and 3.

Table 2. Fitting parameters for Pd-H

χ_{HH}	ϕ_{HH}	δ_{HH}	β_{HH}	η_{HH}	ρ_{HH}
0.95250	0.18342	8.04999	8.75332	0.21342	17.4790
r_{HH}	f_H	F_{HH}			
1.50834	3.53865	2.38746			

Table 3. Fitting parameters for the cross-pair potential

ϕ_{PdH}	δ_{PdH}	β_{PdH}	r_{PdH}
0.32216	4.72446	2.52810	1.20231

3. SIMULATION RESULTS

3.1 EAM functions

EAM functions used in the simulation are plotted in Fig. 2. Figure 2(a) shows well-behaved embedding functions for palladium and hydrogen that reach a minimum at comparable electron densities. The Pd-Pd and H-H pair potentials are shown in Fig. 2(c). The decay of the electron density functions shown in Fig. 2(b) appears reasonable and similar for both palladium and hydrogen over the atomic separation distance range commonly encountered in simulations.

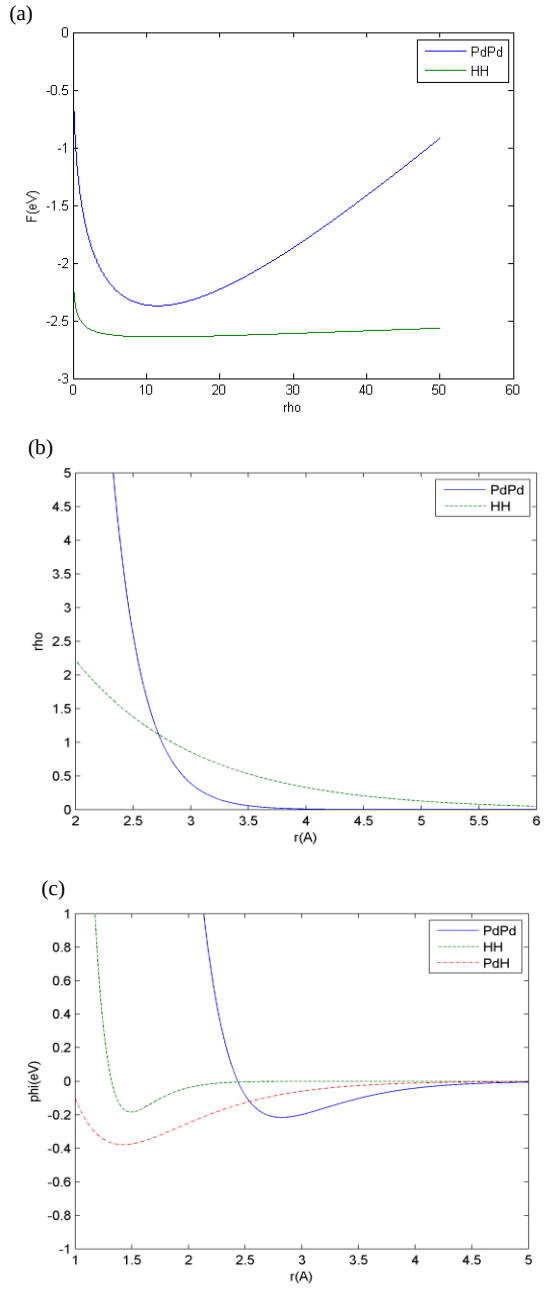

Figure 2. EAM function curves for (a) Embedding function, (b) electron density, and (c) pair potential functions.

3.2 Shear modulus and elastic constant C_{44}.

Shear modulus C' and C_{44} predicted by the EAM potential are plotted in Fig. 3. Trend curves are also plotted. DFT calculations showed that C' increases monotonically as the hydrogen concentration increases, which is opposite to the trend seen in our simulation results. However, Schwarz et al. performed more recent measurements for PdH_x using ultrasonic experimental techniques [16]. In this paper, the authors observe complex

behavior for C' as shown in Fig. 3. While these graphs only show measured data for H concentrations outside of the alpha-beta miscibility gap, it is apparent that the trends predicted in our simulations are consistent with those presented by Schwarz et al. where maximum shear modulus was observed at 0.6 H-composition and C44 is decreasing as the H-composition increases[16].

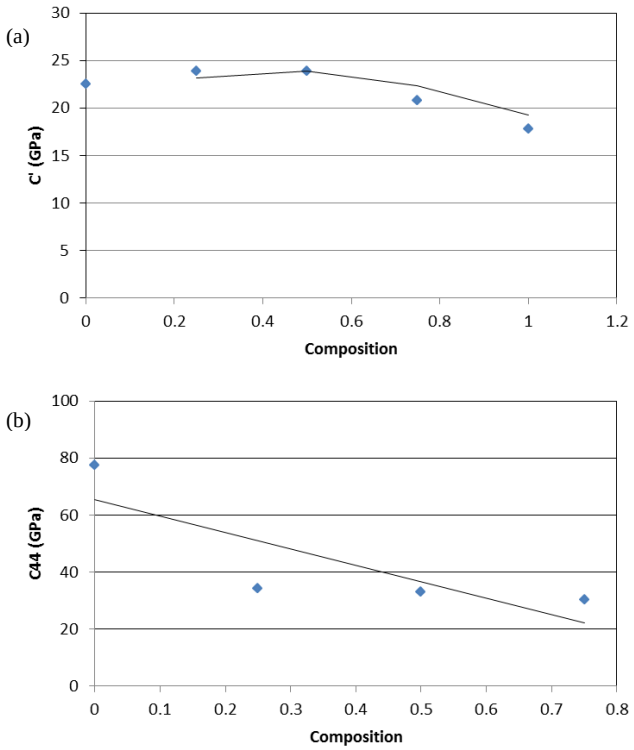

Figure 3. Shear modulus (a) C' and (b) C_{44} predicted by EAM potential function

3.3 Equilibrium lattice constants and cohesive energies

Molecular simulations were conducted based on this potential for various OC structures as a function of composition using a crystal system containing 4×4×4 fcc unit cells. The predicted equilibrium lattice constant and cohesive energy are listed in Table 4. The predicted equilibrium lattice spacing as a function of composition is shown as solid dots in Fig. 4 for the OC PdHx structure. For comparison, the experimental value is shown as the shirt dashed line [17]. The predicted values of lattice constant are in good agreement with experimental result.

Table 4. Predicted values of lattice constant a (Å), cohesive energy E_c (eV/atom).

Structure	a	Ec
$PdH_{0.0}$	3.89	-3.91
$PdH_{0.185}$	3.94	-3.89
$PdH_{0.378}$	3.98	-3.84
$PdH_{0.784}$	4.04	-3.74
$PdH_{1.0}$	4.07	-3.68

3.4 Energetically preferable interstitial sites

Experimental observations showed that interstitial hydrogens in a PdH_x alloy at high concentrations preferentially lie at

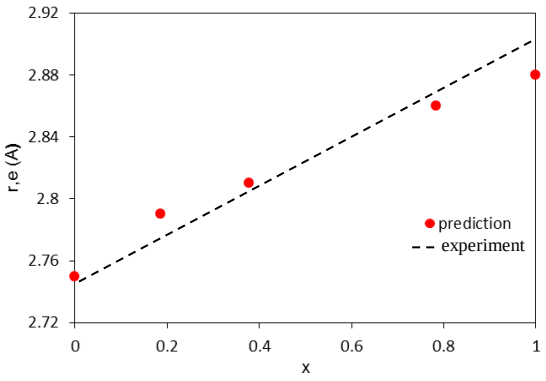

Figure 4. Lattice spacing as a function of composition for OC lattices.

octahedral sites. Hydrogen site selection has proven to be a major hurdle in the development of an accurate inter-atomic potential. Hydrogen can be continuously pumped into the palladium lattice as the surrounding hydrogen gas pressure is increased. As the hydrogen content increases, the solid solution first forms a low hydrogen concentration α phase and then a high concentration, but more defective β phase. In both α and β phases, palladium atoms fully occupy fcc lattices whereas hydrogen atoms partially occupy the octahedral interstitial sites of the palladium lattice. To verify this, Molecular Dynamics (MD) simulation utilizing our EAM potential was conducted on a 4×4×4 unit cells of PdH octahedral structure, utilizing the MD open source code LAMMPS. An NVT ensemble with N equal 512 and T equal 1K was applied during the MD simulation.

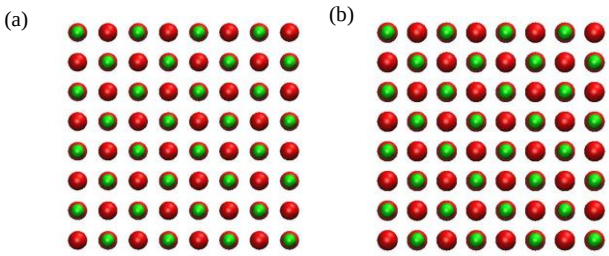

Figure 5. Energy Minimization of PdH using EAM potential. Atomic configuration (a) before minimization and (b) after minimization

It is known that the octahedral site is energetically favorable to the tetrahedral site [18]. To test the energy stability, ideal locations of hydrogen atom were slightly perturbed and the MD simulation was conducted. The energy minimization of the PdH alloy shows that H atoms return to energetically preferable octahedral sites, as shown in Fig. 5 (b).

4. CONCLUSION

Analytical EAM potentials have been developed and tested. This potential is suitable for any composition of the Pd-H system. It predicts the lattice constant, cohesive energy, and elastic properties for a variety of structures. The EAM potential function used is capable of describing the behavior of the Pd-H system.

REFERENCE

[1] R. Lasser: *Tritium and Helium-3 in Metals*, Vol. 9 (Springer-Verlag, Berlin, 1989).

[2] M.S. Ortman, L.K. Heung, A. Nobile, and R.L. Rabun: Tritium processing at the Savannah River site—Present and future. *J. Vac. Sci. Technol., A* **8**(3), 2881 (1990).

[3] R. Povel, K. Feucht, W. Gelse, and G. Withalm: Hydrogen fuel for motorcars. *Interdiscip. Sci. Rev.* **14**(4), 365 (1989).

[4] *Transition Metal Hydrides*, edited by E.L. Muetterties (Marcel Dekker, New York, 1971).

[5] W.M. Mueller, J.P. Blackledge, and G.G. Libowitz: *Metal Hydrides* (Academic Press, New York, 1968).

[6] L.M. Hale, B.M. Wong, J.A. Zimmerman and X.W. Zhou: *Modeling and Simulation in Materials Science and Engineering*. **21**, 045004 (2013).

[7] Knapton A G 1977 Palladium alloys for hydrogen diffusion membranes *Platinum Met. Rev.* **21** 44–50.

[8] Wolf, R. J., Lee, M. Y., and Davis, R. C. Pressure-composition isotherms for palladium hydride, *Physical Review Letter*, Vol. 48, No. 17, 12415-12418 (1993).

[9] S.M. Foiles and J.J. Hoyt: *Computer Simulation of Bubble Growth in Metals Due to He* (Sandia National Laboratories, (2001).

[10] J.A. Zimmerman: *Computer Simulation of Boundary Effects on Bubble Growth in Metals Due to He* (Sandia National Laboratories, *(*2003)

[11] Daw, M. and Baskes, M. Semiempirical, quantum mechanical calculation of hydrogen embrittlement in metals, *Physical Review Letter*, Vol. 50, No. 17, 1285–1288 (1983).

[12] Park, Y. H. and Hijazi, I. A. Simple analytic embedded atom potential for FCC materials: Int. J. Microstructure and Materials Properties, 6(5), 378-396 (2011).

[13] Puska, J., Nieminen, R.M. and Manninen, M. Atoms embedded in an electron gas: immersion energies, *Physical Review B*, Vol. 24, No. 6, pp.3037–3047 (1981).

[14] A. Prince. Alloy Phase Equilibria. Elsevier Publishing Company, Amsterdam, 1966.

[15] Richard A. Swalin. Thermodynamics of Solids. John Wiley & Sons, New York, 1972.

[16] R.B. Schwarz, H.T. Bach, U. Harms, and D. Tuggle. Elastic properties of Pdhydrogen,Pd-deuterium and Pd-tritium single crystals. Acta Materialia, 53:569–580, 2005.

[17] Y. Sakamoto, K. Yuwasa, and K. Hirayama. X-ray investigation of the absorption of hydrogen by several palladium and nickel solid solution alloys. *J. Less-Comm. Metals* **88,** 115 (1982).

[18] X. W. Zhou and J.A. Zimmerman. An embedded-atom method interatomic potential for PdH alloys. J. Mater. Res., 23(3), 704-718. 2008.